

Growing the Gas Giant Planets by the Gradual Accumulation of Pebbles

Harold F. Levison¹, Katherine A. Kretke¹, and Martin J. Duncan²

¹ *Southwest Research Institute and NASA Solar System Exploration Research Virtual Institute, 1050 Walnut St, Suite 300, Boulder, Colorado 80302, USA*

² *Department of Physics, Engineering, and Astronomy, Queen's University, Kingston, Ontario K7L 3N6, Canada*

Prepared for *Nature*

July 5, 2018

It is widely held that the first step in forming the gas giant planets, such as Jupiter and Saturn, is to form solid ‘cores’ of roughly $10 M_{\oplus}$ [1, 2]. Getting the cores to form before the solar nebula dissipates ($\sim 1-10$ Myr [3]) has been a major challenge for planet formation models [4, 5]. Recently models have emerged in which ‘pebbles’ (centimeter- to meter-size objects) are first concentrated by aerodynamic drag and then gravitationally collapse to form 100 — 1000 km objects [6, 7, 8, 9]. These ‘planetesimals’ can then efficiently accrete leftover pebbles [10] and directly form the cores of giant planets [11, 12]. This model known as ‘pebble accretion’, theoretically, can produce $10 M_{\oplus}$ cores in only a few thousand years [11, 13]. Unfortunately, full simulations of this process [13] show that, rather than creating a few $10 M_{\oplus}$ cores, it produces a population of hundreds of Earth-mass objects that are inconsistent with the structure of the Solar System. Here we report that this difficulty can be overcome if pebbles form slowly enough to allow the planetesimals to gravitationally interact with one another. In this situation the largest planetesimals have time to scatter their smaller siblings out of the disk of pebbles, thereby stifling their growth. Our models show that, for a large, and physically reasonable region of parameter space, this typically leads to the formation of one to four gas giants between 5 and 15 AU in agreement with the observed structure of the Solar System.

Our models consist of a series of computer simulations that follow the evolution of a population of objects in a disk around the Sun. The solar composition disk has surface density distribution $\Sigma \propto r_{\text{AU}}^{-1}$, where r_{AU} is the distance from the Sun, and consists of both gas and solids. We assume that an initial population of planetesimals, which follow the surface density of the disk, form quickly and thus exist at the beginning of our simulations. These planetesimals contain only a small fraction of the mass of solids available (a free

parameter of our models). Pebbles either also existed at the beginning of the simulation, or are allowed to form over some period of time (again a free parameter) starting at the beginning of the calculation. The evolution of this system is followed numerically and includes the effects of gravitational interactions, interactions between bodies in the disk and the gas (although nebular tidal migration is neglected), accretion (including enhancements due to the aerodynamic drag on pebbles; e.g. Ref. [11]), and collisional fragmentation. Details of our setup and numerical techniques are described in the *Methods Section*.

In Figure 1 we present the results of two different simulations that employ the same parameters except for the method of pebble formation. In the first (Figure 1a), we assume that the pebbles are leftovers of planetesimal formation and thus they exist at the beginning of the simulation. Note the fast accretion times — embryos (defined to be objects that grow significantly) evolved from roughly the mass of Pluto to that of the Earth in only 1000 years! However, even though Earth-mass embryos form quickly, this simulation does not reproduce the Solar System because rather than forming a few cores, it creates ~ 100 Earth-mass objects. These objects subsequently scatter one another to high-eccentricity, high-inclination orbits, stalling growth. This result is clearly inconsistent with observations. Ref. [13] finds that this is a generic outcome for this type of pebble accretion simulations and thus it could not have occurred in the Solar System. It is indicative of the results one would achieve if the dynamical interactions between planetesimals is neglected (which we refer to as the standard model).

In Figure 1b, we employ a substantial modification to the pebble accretion theory where we couple an extended timescale for pebbles formation (a conjecture supported both by the observed presence of cm to mm-sized grains, which are expected to drift rapidly out of protoplanetary disks, in disks of a wide variety of ages; e.g. Ref.[14] and theoretical models of pebble formation [15]) to the dynamical stirring due to planetesimal self-gravity (so-called

viscous stirring [16]). The behavior of this simulation is radically different from that in Figure 1a in that, rather than producing a large population of Earth-mass objects, a few giant planets form. Only 5 objects grow to $1 M_{\oplus}$ or larger in this simulation, and there are two gas giants at 10 Myr. Also, note that the timescale for growth is very different in the two calculations. The first Earth-mass object grows in 1000 years in the standard pebble accretion run, as opposed to taking slightly over 400,000 years in this simulation. In the latter case, the growth time is determined by the rate at which pebbles were created.

The outcomes of the two simulations are remarkably different because, in the Figure 1b simulation only the most massive embryos are able to accrete a significant amount of pebbles. This is due to the fact that the embryos grow slowly enough in this model that they can gravitationally interact with one another as they accrete the pebbles. This viscous stirring has two effects on the embryo's accretion rates. First, it increases the relative velocities and thus decreases the capture cross-section (*c.f. Methods Section*, Eq. 4). More importantly, encounters between embryos lead to increases in the inclinations, i , of the embryos and thus the distances they travel above and below the disk midplane. Once the inclinations of the embryos become larger than that of the aerodynamically damped pebbles, the embryos spend much of their time above or below the location where the bulk of the pebbles lie. This effectively starves them and stifles their growth. Due to the role of viscous stirring in determining the outcome in these simulations, we refer to this process as *viscously stirred pebble accretion (VSPA)*.

Figure 2 illustrates this effect. In the standard pebble accretion model, the system inclinations remain small and thus all the planetesimals can grow. This because the timescale for viscous stirring is longer than that of the growth. In this case it can be shown (*c.f. Methods Section*) that $dM_e/dt \propto M_e^{\beta}$ and $\beta \ll 1$. The small value of β implies that smaller embryos can catch up with larger ones, leading to a population of like-sized objects.

However, the dynamical evolution of the system is very different in the VSPA simulation. Here viscous stirring can act thereby leading to an increase of inclinations. The magnitude of this increase is set by the mass of the largest embryo — note the increase with time of both the inclination of the smaller embryos and the largest embryo mass in Figure 2b. Initially the inclinations of the embryos are smaller than those of the pebbles, but by 3000 years, most of the smaller embryos begin to spend a significant amount of time above or below the pebbles.

The time at which embryos are excited out of the swarm of pebbles can be estimated with a simple calculation. The inclinations of the pebbles are set by the balance between turbulent excitation and aerodynamic drag in the disk. For our example, the average pebble inclination is 0.0016 radians. Given enough time, a population of embryos will stir one another to the point where their relative velocities are comparable to their surface escape velocities. Since $i \sim v_{rel}/v_c$, even if we assume objects do not grow, our population of planetesimals should reach inclinations of ~ 0.06 — significantly larger than that of the pebbles. As a result, this effect should be important during much of our simulation. Indeed, Figure 2 shows that most of the embryos in the system are in this state after only ~ 3000 years.

The exception is the most massive embryos (Figure 2b), which tend to have low inclinations as a result of a combination of gravitational interactions with smaller planetesimals (so-called dynamical friction [16, 17]) and with the gas (so-called Type I inclination damping [18]). As a result, the larger embryos grow relatively quickly while the smaller embryos grow very slowly, if at all. Recall that the standard model of pebble accretion formed a large number of planets because $\beta < 1$, which allowed smaller embryos to catch up with larger ones. Figure 3 shows the relationship between dM_e/dt and M_e in our fiducial VSPA run as the system evolves. At early times, β is slightly larger than 1, leading to a few embryos becoming dominate in the population. When the largest objects in the system have masses between

$\sim 8 \times 10^{-3} M_{\oplus}$ and $\sim 0.02 M_{\oplus}$ their equilibrium inclinations decrease, leading to a spurt of growth where β is large (~ 4). This allows a small number of embryos to become separated in mass from the rest, and explains why only a small number of embryos become massive enough to become giant planet cores. Indeed, for the small embryos, dM_e/dt decreases with time because of their increasing inclinations (see Figure 2). However for $M_e \gtrsim 0.02 M_{\oplus}$, β becomes small again as the strongly damped, large embryos accrete in the same manner as in the standard pebble accretion scenario. This last phase is important because it forces these proto-cores to have similar masses as they grow. Thus, they all reach the mass where they can directly accrete gas at roughly the same time. This last phase might also explain why the four cores of the giant planets likely originally had similar masses. Two gas giants grow in our fiducial simulation (Jupiter and Saturn?). By varying parameters in the models, our systems produced between 0 and 4 gas giants. Results of the simulations can be found in Extended Data Tables 1 and 2.

There is another constraint that any model of giant planet formation in the Solar System must satisfy in order to be considered a success. The distribution of small bodies in the outer Solar System indicates that the orbits of the giant planets moved substantially after they formed [19, 20, 21]. In particular, Uranus and Neptune likely formed within 15 or 20 AU of the Sun and were delivered to their current orbits by either a smooth migration [20] or a mild gravitational instability [21]. Both processes require that a population of planetesimals existed on low-eccentricity orbits beyond the giant planets after the planets finished forming. This population must have: a) not formed planets, and b) survived the planet formation process relatively unscathed. To evaluate this constraint in our simulations, we placed 5 planetesimals with radii similar to Pluto ($s = 1350$ km) on circular, co-planar orbits with semi-major axes between 20 and 30 AU. None of these objects grew in our fiducial simulation and they all survived on orbits with eccentricities less than 0.07 (see the *Methods Section*

for how this varies with disk parameters). Therefore, the process of viscously stirred pebble accretion reproduces the observed structure of the outer Solar System: two gas giants, a few icy planets, and a disk of planetesimals into which the ice giants can migrate.

References

- [1] Mizuno, H., Nakazawa, K. & Hayashi, C. Instability of a gaseous envelope surrounding a planetary core and formation of giant planets. *Progress of Theoretical Physics* **60**, 699–710 (1978).
- [2] Pollack, J. B. *et al.* Formation of the Giant Planets by Concurrent Accretion of Solids and Gas. *Icarus* **124**, 62–85 (1996).
- [3] Haisch, K. E., Lada, E. A. & Lada, C. J. Disk Frequencies and Lifetimes in Young Clusters. *Astrophys. J. Lett.* **553**, L153–L156 (2001).
- [4] Goldreich, P., Lithwick, Y. & Sari, R. Final Stages of Planet Formation. *Astrophys. J.* **614**, 497–507 (2004).
- [5] Levison, H. F., Thommes, E. & Duncan, M. J. Modeling the Formation of Giant Planet Cores. I. Evaluating Key Processes. *Astron. J.* **139**, 1297–1314 (2010).
- [6] Cuzzi, J. N., Hogan, R. C., Paque, J. M. & Dobrovolskis, A. R. Size-selective Concentration of Chondrules and Other Small Particles in Protoplanetary Nebula Turbulence. *Astrophys. J.* **546**, 496–508 (2001).
- [7] Youdin, A. N. & Goodman, J. Streaming Instabilities in Protoplanetary Disks. *Astrophys. J.* **620**, 459–469 (2005).

- [8] Johansen, A. *et al.* Rapid planetesimal formation in turbulent circumstellar disks. *Nature* **448**, 1022–1025 (2007).
- [9] Youdin, A. N. On the Formation of Planetesimals Via Secular Gravitational Instabilities with Turbulent Stirring. *Astrophys. J.* **731**, 99 (2011).
- [10] Ormel, C. W. & Klahr, H. H. The effect of gas drag on the growth of protoplanets. Analytical expressions for the accretion of small bodies in laminar disks. *Astron. Astrophys.* **520**, A43 (2010).
- [11] Lambrechts, M. & Johansen, A. Rapid growth of gas-giant cores by pebble accretion. *Astron. Astrophys.* **544**, A32 (2012).
- [12] Lambrechts, M. & Johansen, A. Forming the cores of giant planets from the radial pebble flux in protoplanetary discs. *Astron. Astrophys.* **572**, A107 (2014).
- [13] Kretke, K. A. & Levison, H. F. Challenges in Forming the Solar System’s Giant Planet Cores via Pebble Accretion. *Astron. J.* **148**, 109 (2014).
- [14] Ricci, L. *et al.* Dust properties of protoplanetary disks in the Taurus-Auriga star forming region from millimeter wavelengths. *Astron. Astrophys.* **512**, A15+ (2010).
- [15] Birnstiel, T., Klahr, H. & Ercolano, B. A simple model for the evolution of the dust population in protoplanetary disks. *Astron. Astrophys.* **539**, A148 (2012).
- [16] Stewart, G. R. & Wetherill, G. W. Evolution of planetesimal velocities. *Icarus* **74**, 542–553 (1988).
- [17] Ida, S. Stirring and dynamical friction rates of planetesimals in the solar gravitational field. *Icarus* **88**, 129–145 (1990).

- [18] Ward, W. R. Protoplanet Migration by Nebula Tides. *Icarus* **126**, 261–281 (1997).
- [19] Fernandez, J. A., Ip, W.-H. Some dynamical aspects of the accretion of Uranus and Neptune - The exchange of orbital angular momentum with planetesimals. *Icarus* **58**, 109-120 (1984).
- [20] Malhotra, R. The Origin of Pluto’s Orbit: Implications for the Solar System Beyond Neptune. *Astron. J.* **110**, 420–+ (1995).
- [21] Tsiganis, K., Gomes, R., Morbidelli, A. & Levison, H. F. Origin of the orbital architecture of the giant planets of the Solar System. *Nature* **435**, 459–61 (2005).

Acknowledgements

This work was supported by an NSF Astronomy and Astrophysics Research Grant (PI Levison). We would like to thank A. Johansen, M. Lambrechts, A. Morbidelli, D. Nesvorny, and C. Ormel for useful discussions.

1 Author Contributions

H.F.L. and K.A.K. jointly conceived of the paper and carried out the bulk of the numerical and semi-analytic calculations. M.D. developed a semi-analytic model of viscous stirring and growth rates in a population distribution. All authors contributed to the discussion of the results and to the crafting of the manuscript.

Author Information

The authors declare no competing financial interests. Correspondence and requests for materials should be addressed to hal@boulder.swri.edu

Figure Legends

Methods

Computational Methods: LIPAD

For this work we have employed a particle based Lagrangian code (known as LIPAD, Lagrangian Integrator for Planetary Accretion and Dynamics) that can follow the dynamical/collisional/accretional evolution of a large number of planetesimals through the entire growth process to become planets. For full details about the code and extensive test suites see Ref. [22]. For details about how pebble accretion is implemented in the code see Ref. [13], but we summarize the most relevant attributes of the code here.

LIPAD is built on top of the N-body integrator SyMBA [23]. In order to handle the very large number of sub-kilometer objects required by many simulations, LIPAD utilizes a concept known as *tracer particles*. Each tracer represents a large number of small bodies with roughly the same orbit and size, and is characterized by three numbers: the physical radius, the bulk density, and the total mass of the disk particles represented by the tracer. LIPAD employs statistical algorithms that follow the dynamical and collisional interactions between the tracers. When a tracer is determined to have been struck by another tracer, it is assigned a new radius according to the probabilistic outcome of the collision based on a fragmentation law by Ref. [24], using the ice parameters $Q_0 = 7 \times 10^7 \text{ erg g}^{-1}$, $B = 2.1 \text{ erg cm}^3 \text{ g}^{-2}$, $a = -0.45$

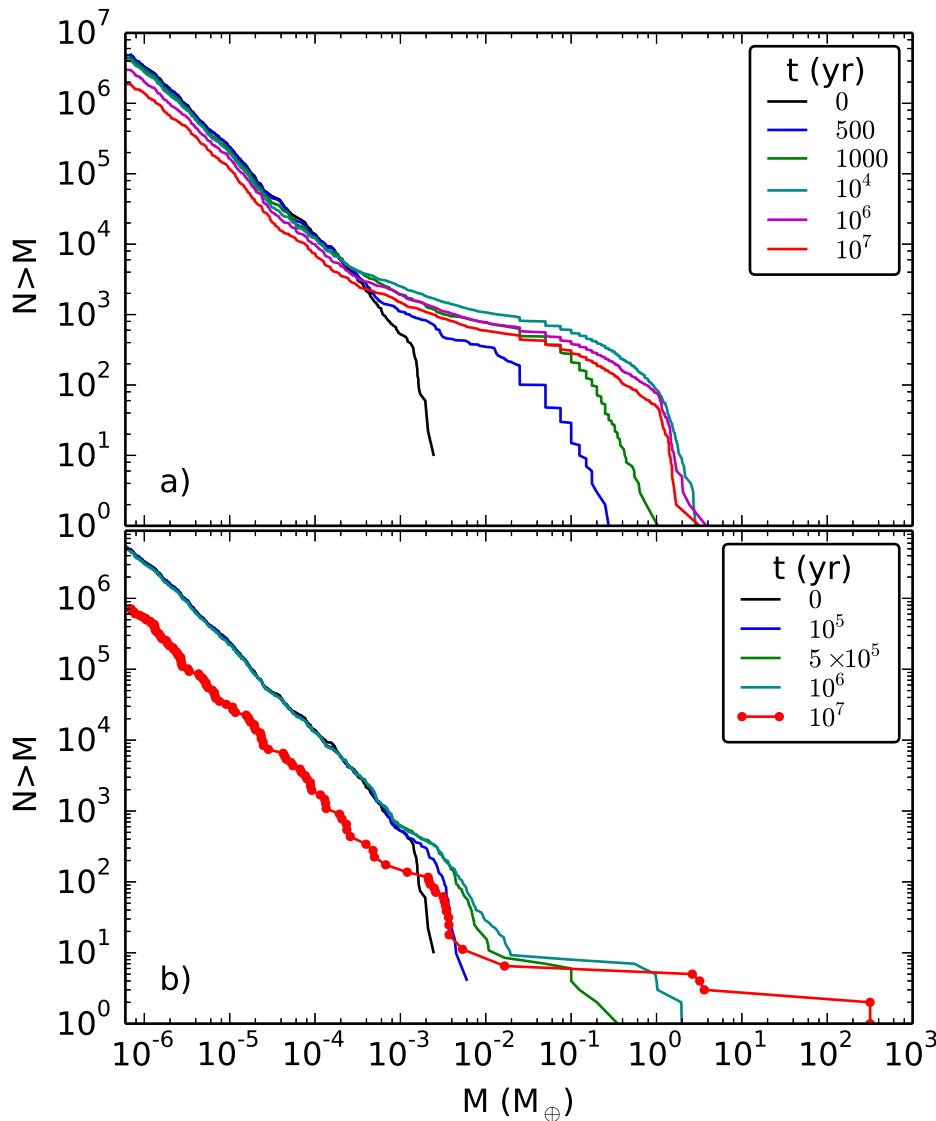


Figure 1: **The cumulative mass distribution of planetesimals and embryos.** The growth of planetary embryos in our simulation as illustrated by cumulative mass distributions shown at various times (indicated by color; see the legend). **a)** An example of standard pebble accretion — all pebbles were in existence at the beginning of the simulation. This is similar to Ref. [13]. **b)** An example with the same disk parameters as (a), but where the pebbles formed over the lifetime of the disk.¹ This system formed two gas giants and three icy planets with masses between 2 and 4 M_{\oplus} . The icy planets are on crossing orbits at the end of the simulation (10 Myr) and thus their number and masses would likely change as the calculation were run to completion. *A movie version of this figure is available in the supplementary material.*

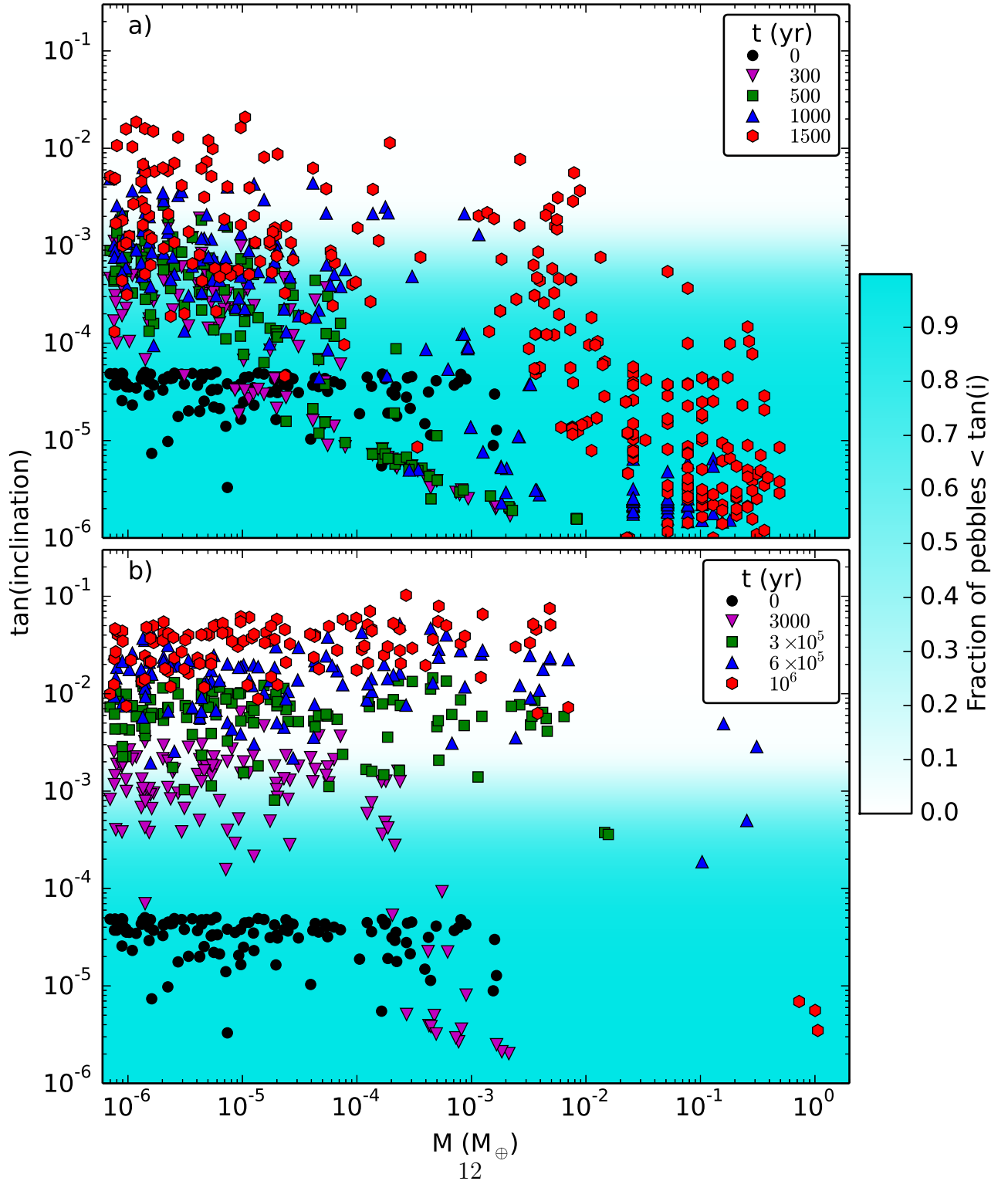


Figure 2: **The vertical distribution of pebbles and embryos.** A comparison between the vertical distribution, as represented by $\tan(i)$, of pebbles and embryos in the simulations shown in Figure 1. The embryos are shown as dots in the figure, where their color indicates the time within the simulation (see legend). Since different simulations exhibit

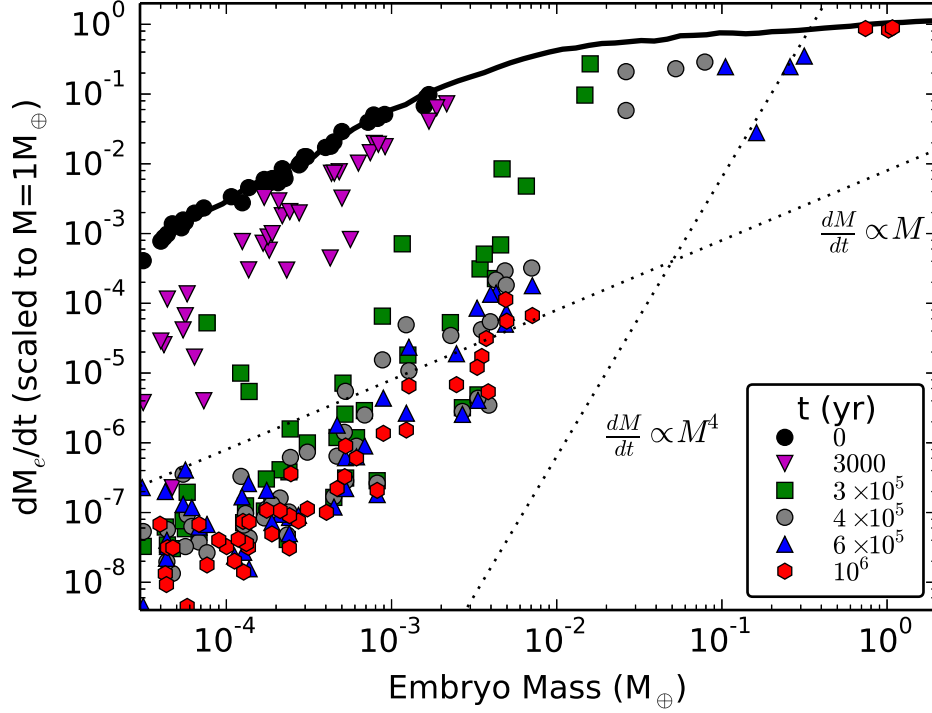


Figure 3: **Embryo growth rate as a function of mass.** The temporal evolution of the relationship between embryo growth rate (dM_e/dt) and mass (M_e). The dots show our fiducial VSPA simulation (Figure 1b), where their color indicates the time within the simulation (see legend). The solid curve is from the standard pebble accretion run in Figure 1a. These values were calculated using procedures described in the *Methods Section*. The behavior of the system is determined by the slope of the data in the figure, β (note that this is a log-log plot) at each time. For reference, the dotted lines show $\beta = 1$ and $\beta = 4$. For $\beta < 1$, small embryos can catch up with larger ones leading to a population of like-sized objects. For $\beta > 1$ the largest embryos run away from their smaller siblings. See *Methods* section for more details.

and $b = 1.19$. This way, the conglomeration of tracers represents the size distribution of the evolving planetesimal population. In this work, we do not allow our pebbles to collisionally grow or fragment, therefore particles below 1 km in size are not involved in the collisional cascade.

LIPAD also includes statistical algorithms for viscous stirring, dynamical friction, and collisional damping among the tracers. The tracers mainly dynamically interact with the larger planetary mass objects via the normal N -body routines, which naturally follow changes in the trajectory of tracers due to the gravitational effects of the planets and *vice versa*. LIPAD is therefore unique in its ability to accurately handle the mixing and redistribution of material due to gravitational encounters, including gap opening, and resonant trapping, while also following the fragmentation and growth of bodies. Thus, it is well suited to follow the evolution of a population of embryos, planetesimals, and pebbles while they gravitationally interact to form planets.

The pebble accretion model follows the prescription in Ref. [10] and is described in detail in Ref. [13]. An overview of the physics follows in the next section.

In the simulations presented here we do not allow the growing planets to migrate via type-I migration [18], although we do include type-I eccentricity damping [25]. We also neglect type-II migration. We calculate the aerodynamic drag on all bodies using the formalism of Ref. [26].

Additionally, as we are interested in the gross evolution of a system after the formation of a potential giant planet core, we have added a simple optional prescription allowing cores to accrete gas envelopes. In order to accrete gas the core size must be above a critical value, which depends on the mass accretion rate of solids onto the core. We follow Ref. [27] to determine when core masses are above the critical value given their current mass accretion rate (assuming a grey opacity of 0.02 times that of the ISM [2]). If this criteria is met then

we grow the planet of mass M_p on the Kelvin Helmholtz timescale (t_{KH}), so that

$$\dot{M}_g = \frac{M_p}{t_{\text{KH}}}. \quad (1)$$

Following Ref. [28] we approximate this timescale as

$$t_{\text{KH}} = 10^9 \left(\frac{M_p}{M_{\oplus}} \right)^{-3} \text{ yrs.} \quad (2)$$

We limit gas accretion to the Bondi accretion rate,

$$\dot{M}_{\text{g,max}} = \frac{4\pi\rho_g G^2 M_p^2}{c_s^3}, \quad (3)$$

where ρ_g is the gas density and c_s is the local sound speed. We note that a major uncertainty in these models is the envelope opacity, which is dominated by the poorly constrained properties of the dust. Varying the opacity dramatically alters both the size of the critical core mass, and perhaps more strikingly, the Kelvin-Helmholtz time. Additionally, we arbitrarily cut off gas accretion when a planet reaches one Jupiter mass instead of including any physics to reduce the accretion of gas after gap opening (e.g. Ref. [29]). Furthermore, we do not include the fact that pebbles will cease accreting onto planetesimal cores once the cores begin perturbing the disk [30]. This effect may prove important in causing some cores to accrete gas sooner, or in allowing cores to grow to larger sizes without accreting gas (creating true Uranus and Neptune analogs). Therefore the end masses of giant planets should be viewed with these caveats in mind.

We also note that while this model includes fragmentation, we have found that the production, and subsequent sweep-up of pebbles (as considered by Ref. [31]) is relatively unimportant in these scenarios. This is due to the assumed relatively low initial mass of planetesimals in our simulations ($17 M_{\oplus}$ between 4 and 15 AU in our fiducial simulation).

Pebble Accretion

Here we present an argument, based on Refs. [10, 11], about why pebbles are effectively accreted by growing planets. If the stopping time (t_s) of a pebble is comparable to the time for it to encounter a growing embryo, then it can be deflected out of the gas stream and lose enough orbital energy to become gravitationally bound to the embryo. After capture, the pebble spirals inward due to aerodynamic drag and is accreted. In this case the collisional cross section for accretion is

$$\sigma_{\text{peb}} \equiv \pi \left(\frac{4GM_e t_s}{v_{\text{rel}}} \right) \exp \left[-2 \left(\frac{t_s v_{\text{rel}}^3}{4GM_e} \right)^\gamma \right], \quad (4)$$

where M_e is the mass of the embryo, v_{rel} is the relative velocity between the pebble and embryo, G is the gravitational constant, and $\gamma = 0.65$ [10]. When the Stokes number of a pebble ($\tau \equiv t_s \Omega_K$, where Ω_K is the local Keplerian frequency) is near unity, this capture radius can be 10^7 times larger than the physical cross section alone (πR_e^2 , where R_e is the radius of the embryo) for Earth-sized planets in the region inhabited by the giant planets.

This process can cause an isolated 1000 km object to grow into a $10 M_\oplus$ core in only a few thousand years [11, 13]. To zeroth order, the accretion rate of an embryo growing by pebble accretion is $dM_e/dt = f_{\text{ac}} \mathcal{R}$, where f_{ac} is the fraction of pebbles that drift into an embryo's orbit that will be accreted (also called the filtering factor, which is a function of σ_{peb} and the spatial distribution of pebbles), $\mathcal{R} = 2\pi r \Sigma_{\text{peb}} v_{\text{rad}}$ is the rate at which pebbles are fed to the embryo, Σ_{peb} is the surface density of pebbles at heliocentric distance r , and v_{rad} is the radial velocity of the pebbles due to aerodynamic drag. Pebbles drift at a velocity

$$v_{\text{rad}} = -2 \frac{\tau}{\tau^2 + 1} \eta v_c, \quad (5)$$

where η is a dimensionless parameter related to the pressure gradient of the gas disk [32] and is on the order of a few times 10^{-3} , and v_c is the local circular velocity of the embryo.

For $\tau \sim 1$, a pebble can spiral through the disk in only a few hundred years. These large values of v_{rad} can lead to huge accretion rates and giant planet cores can potentially grow quickly.

Pebble Formation Model

In this work we utilize a simple prescription to convert dust into pebbles over time. We assume that the gas disk with mass M_g exponentially decays over a timescale t_g , so that

$$\dot{M}_g = -\frac{M_g}{t_g}. \quad (6)$$

Pebbles (with total mass M_{peb}) are formed at a rate proportional to the square of the dust mass (M_d) such that

$$\dot{M}_{\text{peb}} = kM_d^2, \quad (7)$$

where k determines the rate of pebble formation. The dust in the disk will be lost as the gas disk evolves and as pebbles form, yielding a dust evolution of

$$\dot{M}_d = \dot{M}_g \frac{M_d}{M_g} - \dot{M}_{\text{peb}}. \quad (8)$$

This leads to a total rate of pebble production of

$$\dot{M}_{\text{peb}} = \frac{\kappa}{t_g} M_{d,0} \frac{1}{(1 + \kappa)^2} \left(\frac{1}{\exp(t/t_g) - \kappa/(1 + \kappa)} \right)^2, \quad (9)$$

where $\kappa \equiv kt_g M_{d,0}$. Motivated by observations of disks, we take the time constant for pebble production to be large, with a median production timescale near 1 Myr. We assume that all of the pebbles are produced in 3 Myr. For simplicity, we assume that pebbles are randomly created throughout the disk according to the surface density, and the size of the pebbles is determined by the assumed τ , which is constant in each simulation, but varies between calculations.

To test the robustness of our result to the specific assumptions of our pebble formation model, we modified it in two different ways for the runs shown in the Extended Data Tables. In some runs we allow the pebbles to grow as they drift inwards by sweeping up dust. Their growth rate is thus

$$\frac{dm}{dt} = \rho_d \pi r_{\text{peb}}^2 v_{\text{rel}}, \quad (10)$$

where ρ_d is the dust mass (which is depleted as pebbles are formed, as dust is swept up, and as the gaseous disk evolves), r_{peb} is the size of the pebble, and v_{rel} is the relative velocity between the pebble and the dust (which is assumed to be perfectly coupled to the gas).

In other runs, we assume a model of pebble formation consistent with the inside out manner suggested by Ref. [15]. We used the implementation as described in Ref. [12] and had a wave of pebble formation which moves outwards as a function of time. In particular, the radius at which pebbles are generated (r_g) at time t is

$$r_g(t) = \left(\frac{3}{16}\right)^{1/3} (GM_*)^{1/3} (\epsilon_d Z_0)^{2/3} t^{2/3}, \quad (11)$$

where Z_0 is the metallicity of the disk and ϵ_d encapsulates the efficiency of particle growth. We modify ϵ_d to adjust the timescale of pebble formation. We found that so long as the coagulation coefficient is small enough that the timescale for pebble formation is long, we can get results that are generally similar to our fiducial model in which pebbles form randomly.

Model Parameters and Simulation Statistics

Since we are interested in building the gas giant planets, we study the growth of planetesimals spread from 4 to 15 AU. As we integrate the simulation forwards, pebbles are formed between 4 and 30 AU. Each system was evolved 10 Myr using LIPAD. Extended Data Tables 1 and 2 list the 42 simulations that we have completed in our investigation of giant planet formation. The eight important parameters that were varied are:

1. The surface density of the gas disk at 1 AU, Σ_0 . In all our simulations we used a surface density distribution of $\Sigma = \Sigma_0 r_{\text{AU}}^{-1}$ [33], where r_{AU} is the heliocentric distance in AU. For the fiducial simulation, $\Sigma_0 = 7200 \text{ g/cm}^2$, which is 4 times the surface density of the minimum mass solar nebula at that location [34]. The gas surface density decreases exponentially with a timescale of 2 Myr [3, 35].
2. We employ a flaring gas disk with a scale height $h = 0.047 r_{\text{AU}}^q \text{ AU}$. We used two values for q : 1.25 from Ref. [34] and 9/7 from Ref. [36]. The later was used in our fiducial run.
3. The size of the largest planetesimal, s_{max} . We draw the initial planetesimals from a distribution of radii, s , of the form $dN/ds \propto s^{-4.5}$ such that s is between 100 km [37] and s_{max} . For our fiducial simulation $s_{\text{max}} = 1350 \text{ km}$, which is slightly larger than Pluto.
4. The fraction of solids in the disk that are initially converted into planetesimals, f_{pl} . For all simulations, we assume a solid-to-gas ratio of 0.01, which includes the contribution of water ice [38], and f_{pl} of the solids are in planetesimals while $(1 - f_{pl})$ are in pebbles. For the fiducial simulation, $f_{pl} = 0.1$, which, if extended to 30 AU, is consistent with the mass of planetesimals needed to subsequently deliver the giant planets to their current orbits [21].
5. The initial Stokes number of a pebble, τ . Note that as pebbles spiral toward the Sun, their Stokes number changes (generally decreases) even when it is assumed that they do not grow. For our fiducial simulation $\tau = 0.6$.
6. The strength of inclination and eccentricity damping due to the gravitational interaction with the gas disk, c_e . We employ the techniques in Ref. [5], which are based on

Ref. [25] and allow for both radial migration and inclination/eccentricity damping. The strength of both processes can be adjusted by varying two dimensionless parameters: c_a and c_e , respectively. All our simulations have $c_a = 0$, meaning there is no Type I migration. For our fiducial simulation $c_e = 0.66$.

7. LIPAD [22], has the option of allowing pebbles to grow by the accretion of dust particles suspended in the gas. The growth rates are calculated using the particle-in-a-box approximation assuming the distribution of dust follows that of the gas, as described above. Our fiducial simulation has this option disabled.
8. The median time of pebble generation, t_{gen} . For most of our simulations, pebble generation follows the evolution of the gas disk. In this case $t_{\text{gen}} \sim 0.7 \text{ Myr}$. However, in two cases we decreased t_{gen} in order to determine whether it affects our results. We found that the value of t_{gen} is not important as long as it is larger than the viscous stirring timescale of the embryos. Times marked with an asterisk indicate that pebbles were generated in an inside-out manner as described above.

Additionally, all the disks are turbulent with $\alpha = 4 \times 10^{-3}$ [39].

The last five columns in the table present the basic characteristics of our systems. In particular, N^{Gas} is the total number of gas giant planets that formed during each run. It ranges from 0 to 4. Occasionally, a giant planet or two was lost from the system. Although some of these were ejected due to dynamical instabilities, the majority were pushed off the inner edge of our computational domain by their neighbors as the latter accreted gas. Unfortunately, the inner edge of the domain needs to be relatively large because it determines the timestep used in the calculation. The N -body integrator requires that the perihelion passage be temporally resolved, and since the location of the domain's inner boundary determines the smallest perihelion, it also sets the timestep. In order for the calculations to

be practical, we were forced to remove any object with a perihelion distance smaller than 2.7 AU (the location of the snow line). The majority of the lost gas giants would likely have remained in the asteroid belt or migrated into the terrestrial planet region if we had been able to keep them in the calculations. The column labeled N_f^{Gas} gives the number of gas giants remaining in the system at 10 Myr.

Columns (11) and (12) refer to icy objects with masses greater than $1 M_{\oplus}$. Again, N^{ice} and N_f^{ice} are the total number of planets that formed and the number remaining at 10 Myr, respectively. Unlike their larger siblings, the majority of the lost icy planets were ejected from the planetary system, mainly by encounters with growing gas giants. The number of lost ice planets illustrates the fact that the systems becomes violent after the largest cores begin to accrete gas. The last column shows whether the 5 planetesimals we placed on circular, co-planar orbits between 20 and 30 AU (as proxies for the planetesimal disk needed for later planet migration [21]) survived at 10 Myr.

There are a couple of important caveats that must be taken into account to properly interpret the results in the Extended Data Tables. First the parameter space for our calculations is 8-dimensional, and each calculation required many weeks of CPU time. This limited the total number that could be performed. Thus, it was impossible to cover parameter space in a meaningful way. Instead, we surgically approached the problem by choosing a couple of starting locations and varying individual parameters to test their effects. We then moved in a particular direction in parameter space if we believed we would be more likely to produce systems with some desired characteristic. As a result, the distribution of our results seen in the table (for example the number of gas giants) cannot be interpreted as the true distribution that would result if parameter space were uniformly covered.

Our second concern is the crude methods we used to model the direct accretion of gas onto the cores to form gas giants. As discussed above, our simple model for calculating for

the onset of gas accretion and the final mass of planets likely is missing important physics. These limitations mean that, while our calculations show the pebble accretion produces the correct number of giant planet cores on the correct timescales, the details of the evolution of our systems after the gas giants form should be viewed with skepticism.

Generating Figure 3

The data in Figure 3 were generated using the following procedure. We first needed to construct a high resolution distribution of pebbles. This was accomplished by summing the output steps of our integration over all time. Then at each time plotted, we noted the mass and orbit of each embryo. We then generated 1000 clones of each embryo — each with the same semi-major axis, eccentricity, and inclination, but with different orbital angles. For each clone, we calculated its velocity with respect to the pebbles and then σ_{peb} from Eq. (4). From this we estimate the instantaneous accretion rate using the particle-in-a-box approximation, $\dot{M}_e = \rho \sigma_{\text{peb}} v_{\text{rel}}$ where ρ is the local mass density of pebbles. The dots in the figure show the average of the 1000 clones of the instantaneous accretion rates for each embryo.

Code Availability

The calculations presented in this paper were performed using LIPAD, a proprietary software product funded by the Southwest Research Institute and is not publicly available. It is based upon the N-Body integrator SyMBA, which is publicly available at <http://www.boulder.swri.edu/swifter/>

Table 1: **Our completed simulations.** Please see the *Methods Section* for a full description of the columns in this table.

| (1) | (2) | (3) | (4) | (5) | (6) | (7) | (8) | (9) | (10) | (11) | (12) | (13) |
|----------------------|------|------------|----------|--------|-------|------------------|------------------|------------------|--------------------|------------------|--------------------|----------|
| Σ_0 | q | s_{\max} | f_{pl} | τ | c_e | pebbles grow? | t_{gen} | N^{Gas} | N_f^{Gas} | N^{ice} | N_f^{ice} | Disk ok? |
| (g/cm ²) | | (km) | | | | (Y/N) | (Myr) | | | | | (Y/N) |
| 3600 | 9/7 | 1500 | 0.2 | 0.3 | 1 | N | 0.7 | 4 | 2 | 12 | 0 | Y |
| 3600 | 9/7 | 1500 | 0.2 | 0.3 | 1 | N | 0.5 | 4 | 3 | 14 | 0 | Y |
| 3600 | 9/7 | 1500 | 0.2 | 0.3 | 1 | N | 0.2 | 4 | 3 | 15 | 1 | N |
| 3600 | 9/7 | 1500 | 0.2 | 0.4 | 1 | N | 0.7 | 3 | 1 | 9 | 2 | Y |
| 3600 | 1.25 | 1500 | 0.2 | 3 | 1 | Y | 0.7 | 3 | 2 | 9 | 0 | Y |
| 4050 | 9/7 | 1500 | 0.18 | 0.4 | 1 | N | 0.7 | 4 | 2 | 6 | 1 | Y |
| 4050 | 9/7 | 1500 | 0.18 | 0.5 | 1 | N | 0.7 | 3 | 3 | 7 | 0 | Y |
| 4050 | 9/7 | 1500 | 0.18 | 0.6 | 1 | N | 0.7 | 4 | 4 | 9 | 0 | Y |
| 4500 | 9/7 | 1500 | 0.16 | 0.3 | 1 | N | 0.7 | 4 | 3 | 13 | 0 | Y |
| 4500 | 9/7 | 1500 | 0.16 | 0.4 | 1 | N | 0.7 | 3 | 2 | 7 | 1 | Y |
| 4500 | 9/7 | 1500 | 0.16 | 0.5 | 1 | N | 0.7 | 3 | 3 | 13 | 0 | N |
| 4500 | 9/7 | 1500 | 0.16 | 0.5 | 0.33 | N | 0.7 | 4 | 2 | 4 | 0 | Y |
| 4500 | 9/7 | 1500 | 0.16 | 0.5 | 0.1 | N | 0.7 | 0 | 0 | 7 | 6 | Y |
| 4500 | 9/7 | 1500 | 0.16 | 0.6 | 1 | N | 0.7 | 2 | 2 | 15 | 3 | N |
| 4500 | 9/7 | 1500 | 0.16 | 0.7 | 1 | N | 0.7 | 0 | 0 | 7 | 7 | Y |
| 4500 | 9/7 | 1500 | 0.16 | 0.9 | 1 | N | 0.7 | 1 | 0 | 1 | 1 | Y |
| 5400 | 1.25 | 1500 | 0.15 | 3 | 1 | Y | 0.7 | 0 | 0 | 5 | 4 | Y |
| 5400 | 1.25 | 1500 | 0.15 | 3 | 1 | Y | 0.7 | 0 | 0 | 6 | 6 | Y |
| 5400 | 1.25 | 1500 | 0.15 | 3 | 0.66 | Y | 0.7 | 0 | 0 | 5 | 5 | Y |
| 5400 | 1.25 | 1500 | 0.15 | 3 | 0.33 | Y | 0.7 | 1 | 1 | 7 | 4 | Y |
| 7200 | 9/7 | 1350 | 0.25 | 0.6 | 1 | N ²³ | 0.7 | 4 | 4 | 10 | 2 | Y |
| 7200 | 9/7 | 1350 | 0.15 | 0.6 | 1 | N | 0.7 | 4 | 4 | 8 | 0 | N |
| 7200 | 1.25 | 1500 | 0.1 | 1 | 1 | Y | 0.7 | 2 | 2 | 11 | 4 | Y |
| 7200 | 1.25 | 1500 | 0.1 | 1 | 0.25 | Y | 0.7 | 3 | 3 | 5 | 1 | Y |
| 7200 | 1.25 | 1500 | 0.1 | 1 | 0 | Y | 0.7 | 2 | 2 | 1 | 0 | Y |

Table 2: More Simulations. This is a continuation of Extended Data Table 1. Please see the *Methods Section* for a full description of the columns in this table.

| (1) | (2) | (3) | (4) | (5) | (6) | (7) | (8) | (9) | (10) | (11) | (12) | (13) |
|----------------------|------|------------|----------|--------|-------|------------------|------------------|------------------|--------------------|------------------|--------------------|----------|
| Σ_0 | q | s_{\max} | f_{pl} | τ | c_e | pebbles grow? | t_{gen} | N^{Gas} | N_f^{Gas} | N^{ice} | N_f^{ice} | Disk ok? |
| (g/cm ²) | (km) | | | | | (Y/N) | (Myr) | | | | | (Y/N) |
| 900 | 9/7 | 1500 | 0.8 | 0.1 | 0.66 | N | 0.9* | 0 | 0 | 21 | 15 | Y |
| 900 | 9/7 | 1500 | 0.8 | 0.1 | 0.66 | N | 1.3* | 0 | 0 | 17 | 14 | Y |
| 1800 | 9/7 | 1500 | 0.4 | 0.1 | 0.66 | N | 0.9* | 5 | 4 | 8 | 0 | N |
| 1800 | 9/7 | 1500 | 0.4 | 0.1 | 0.66 | N | 1.3* | 3 | 3 | 6 | 0 | N |
| 3600 | 9/7 | 1500 | 0.2 | 0.1 | 0.66 | N | 0.9* | 7 | 5 | 12 | 0 | N |
| 3600 | 9/7 | 1500 | 0.2 | 0.1 | 0.66 | N | 1.3* | 6 | 4 | 9 | 0 | N |
| 3600 | 9/7 | 1500 | 0.2 | 0.1 | 0.66 | N | 0.4* | 4 | 3 | 9 | 0 | N |
| 3600 | 9/7 | 1500 | 0.2 | 0.6 | 0.66 | N | 0.9* | 5 | 3 | 6 | 0 | N |
| 3600 | 9/7 | 1500 | 0.2 | 0.6 | 0.66 | N | 0.4* | 2 | 2 | 11 | 4 | Y |
| 7200 | 9/7 | 1500 | 0.1 | 0.6 | 0.66 | N | 0.4* | 3 | 1 | 10 | 1 | N |
| 7200 | 9/7 | 1500 | 0.1 | 0.6 | 0.66 | N | 0.9* | 4 | 3 | 6 | 0 | N |
| 7200 | 9/7 | 1500 | 0.1 | 0.6 | 0.66 | N | 1.3* | 5 | 3 | 5 | 1 | N |

Extended Data Legends

References

- [22] Levison, H. F., Duncan, M. J. & Thommes, E. A Lagrangian Integrator for Planetary Accretion and Dynamics (LIPAD). *Astron. J.* **144**, 119–138 (2012).
- [23] Duncan, M. J., Levison, H. F. & Lee, M. H. A Multiple Time Step Symplectic Algorithm for Integrating Close Encounters. *Astron. J.* **116**, 2067–2077 (1998).
- [24] Benz, W. & Asphaug, E. Catastrophic Disruptions Revisited. *Icarus* **142**, 5–20 (1999).
- [25] Papaloizou, J. C. B. & Larwood, J. D. On the orbital evolution and growth of proto-planets embedded in a gaseous disc. *Astronomy* **315**, 823–833 (2000).
- [26] Adachi, I., Hayashi, C. & Nakazawa, K. The gas drag effect on the elliptical motion of a solid body in the primordial solar nebula. *Progress of Theoretical Physics* **56**, 1756–1771 (1976).
- [27] Rafikov, R. R. Atmospheres of Protoplanetary Cores: Critical Mass for Nucleated Instability. *Astrophys. J.* **648**, 666–682 (2006).
- [28] Ida, S. & Lin, D. N. C. Toward a Deterministic Model of Planetary Formation. IV. Effects of Type I Migration. *Astrophys. J.* **673**, 487–501 (2008).
- [29] Dobbs-Dixon, I., Li, S. L. & Lin, D. N. C. Tidal Barrier and the Asymptotic Mass of Proto-Gas Giant Planets. *Astrophys. J.* **660**, 791–806 (2007).
- [30] Lambrechts, M., Johansen, A. & Morbidelli, A. Separating gas-giant and ice-giant planets by halting pebble accretion. *Astron. Astrophys.* **572**, A35 (2014).

- [31] Chambers, J. E. Giant planet formation with pebble accretion. *Icarus* **233**, 83–100 (2014).
- [32] Nakagawa, Y., Sekiya, M. & Hayashi, C. Settling and growth of dust particles in a laminar phase of a low-mass solar nebula. *Icarus* **67**, 375–390 (1986).
- [33] Andrews, S. M., Wilner, D. J., Hughes, A. M., Qi, C. & Dullemond, C. P. Protoplanetary Disk Structures in Ophiuchus. II. Extension to Fainter Sources. *Astrophys. J.* **723**, 1241–1254 (2010).
- [34] Hayashi, C. Structure of the Solar Nebula, Growth and Decay of Magnetic Fields and Effects of Magnetic and Turbulent Viscosities on the Nebula. *Progress of Theoretical Physics Supplement* **70**, 35–53 (1981).
- [35] Hernández, J. *et al.* Spitzer Observations of the λ Orionis Cluster. I. The Frequency of Young Debris Disks at 5 Myr. *Astrophys. J.* **707**, 705–715 (2009).
- [36] Chiang, E. I. & Goldreich, P. Spectral Energy Distributions of T Tauri Stars with Passive Circumstellar Disks. *Astrophys. J.* **490**, 368–376 (1997).
- [37] Morbidelli, A., Bottke, W. F., Nesvorný, D. & Levison, H. F. Asteroids were born big. *Icarus* **204**, 558–573 (2009).
- [38] Lodders, K. Solar System Abundances and Condensation Temperatures of the Elements. *Astrophys. J.* **591**, 1220–1247 (2003).
- [39] Shakura, N. I. & Sunyaev, R. A. Black holes in binary systems. Observational appearance. *Astron. Astrophys.* **24**, 337–355 (1973).